

# Structural and electric properties of $\text{SrZrO}_3$ thin films on different Pt bottom electrodes

Y.K. Lu, C.H. Chen, W. Zhu\*, T. Yu, X.F. Chen

*School of Electrical and Electronic Engineering, Nanyang Technological University, Nanyang Avenue, Singapore 639798, Singapore*

Received 26 November 2003; received in revised form 30 November 2003; accepted 22 December 2003

Available online 6 May 2004

## Abstract

$\text{SrZrO}_3$  thin films were deposited on Pt/Ti/SiO<sub>2</sub>/Si and Pt/TiO<sub>2</sub>/SiO<sub>2</sub>/Si substrates by the metal-organic decomposition technology followed by post-annealing at different temperatures ranging from 550 to 800 °C in flowing oxygen atmosphere. The microstructure characteristics of these films were investigated using X-ray diffraction, Fourier transform infrared reflectivity spectroscopy and scanning electron microscopy. Their dielectric and leakage current characteristics were evaluated by a HP-4284A precision LCR meter and a HP-4155B semiconductor parameter analyzer, respectively. The phase transformation and crystallinity results indicate that the film has amorphous structure with carbonate existing when annealed at 550 °C; however when annealed at 600 °C and above, the carbonate is decomposed and those films crystallize into the Perovskite phase. The dielectric constant of  $\text{SrZrO}_3$  is above 22 with little dispersion in a frequency range from 100 Hz to 1 MHz. The results also indicate that when annealed above 650 °C, the films using Pt/TiO<sub>2</sub>/SiO<sub>2</sub>/Si show much better leakage properties compared with those using Pt/Ti/SiO<sub>2</sub>/Si. And even annealed at 800 °C, the films deposited on Pt/TiO<sub>2</sub>/SiO<sub>2</sub>/Si substrate still have good leakage properties.

© 2004 Elsevier Ltd and Techna Group S.r.l. All rights reserved.

**Keywords:** A. Films; A. Sol–gel processes; C. Electrical properties; E. Capacitors

## 1. Introduction

Perovskite materials are important materials for various functional devices.  $\text{SrZrO}_3$ -based perovskite oxides have been studied because of the interest in their high-temperature protonic conductivity [1,2], promising use in MHD generators [3,4]. Besides these,  $\text{SrZrO}_3$  still has many characteristics which are suitable for high-voltage and high-reliability capacitor applications. Recently,  $\text{SrZrO}_3$  has been investigated as a possible candidate material for high- $K$  gate dielectrics [5].

In order to determine the performance of a dielectric thin film capacitor, bottom electrode is very important because the structural and electrical properties such as leakage current, dielectric properties, surface roughness, and thermal stability are strongly related to the nature and state of the bottom electrode [6,7]. And the best electrode metallization needs to preserve the low resistivity during oxygen anneal-

ing. That is why platinum is one of the mostly used electrode material for electroceramic devices [8]. In addition, in order to ensure good adhesion of this metallization and prevent the formation of Pt silicides at high temperature, a bonding layer of titanium is often deposited between the Pt and silicon substrate [9]. However, the interdiffusion of Ti into Pt at high temperature is a well-known phenomenon [10], which causes rapid oxidation of the Ti layer, followed by the migration of Ti into the Pt film. Hence, the high-temperature behavior of Pt/Ti bottom electrode is crucial for the deposition of dielectric thin films on top of such metal films.

An interesting phenomenon is that the interdiffusion of Ti into Pt caused the formation of TiO<sub>2-x</sub> in the Pt-grain boundaries, encapsulating the Pt surface with an insulating TiO<sub>2</sub> layer [11]. Hence, in this work, in order to protect the Pt electrode from the interdiffusion of Ti, we have prepared Pt/TiO<sub>2</sub> bottom electrode on silicon substrate and investigated the structural and electrical properties of  $\text{SrZrO}_3$  thin films deposited on this substrate by the sol–gel method. These properties are compared to those obtained by using the conventional Pt/Ti/SiO<sub>2</sub>/Si substrate.

\* Corresponding author. Tel.: +65-6790-4541; fax: +65-6792-0415.  
E-mail address: ewzhu@ntu.edu.sg (W. Zhu).

## 2. Experimental

### 2.1. Film preparation

Strontium acetate ( $\text{Sr}(\text{CH}_3\text{COO})_2$ ) and zirconium acetylacetonate ( $[\text{CH}_3\text{COCH}=\text{COCH}_3]_4\text{Zr}$ ) were chosen as the precursors, which were separately and thoroughly dissolved in glacial acetic acid ( $\text{CH}_3\text{COOH}$ ) by stirring at a temperature of  $60^\circ\text{C}$  for 1 h followed by mixing and stirring at room temperature to get a clear and transparent solution with desired mole ratio of  $\text{Sr}:\text{Zr} = 1:1$ . The resulting solution with a concentration of 0.2 M was continuously stirred for 1 h and prepared for thin film deposition. The precursor solution was first spin-coated onto the substrates at 4000 rpm and then baked at  $230$  and  $400^\circ\text{C}$  for 2 min, respectively, in air to remove most organics in the film. After this procedure was repeated three times, the dried films were post-annealed in the furnace at the temperature ranging from  $550$  to  $800^\circ\text{C}$  for 30 min in  $\text{O}_2$  atmosphere. Top electrodes of Pt with a diameter of 0.3 mm were sputtered for electrical measurement.

We have used two kinds of substrate in this study. Pt (150 nm)/Ti (150 nm)/ $\text{SiO}_2$  (500 nm)/Si substrate was commercially purchased. And we obtained Pt (180 nm)/ $\text{TiO}_2$  (110 nm)/ $\text{SiO}_2$  (500 nm)/Si substrate by r.f. sputtering. The Pt/ $\text{TiO}_2$  bilayer was fabricated by a two step deposition process. A 110 nm  $\text{TiO}_2$  was first deposited on the silicon substrate followed by the sputtering of a 180 nm-thick Pt layer.

### 2.2. Film characterization

The organic residuals in thin films were monitored by a Perkin-Elmer 2000 FT-IR spectrometer. The structural development of the  $\text{SrZrO}_3$  films was investigated using a Siemens D5005 X-ray diffractometer with grazing angle  $2^\circ$ . The light source was X-ray  $1.54056 \text{ \AA}$  of  $\text{Cu K}\alpha$  radiation at 40 kV and 40 mA. The scan range of  $2\theta$  was from

$20$  to  $70^\circ$  at a sweep rate  $2^\circ/\text{min}$ . Surface morphology was studied using field-emission scanning electron microscopy (FE-SEM). The dielectric and leakage current characteristics were evaluated by a HP-4284A precision LCR meter and a HP-4155B semiconductor parameter analyzer, respectively.

## 3. Results and discussion

### 3.1. Structural properties

Fig. 1 shows the crystalline structure of the  $\text{SrZrO}_3$  thin films which were deposited on two different kinds of pt-coated silicon substrates and annealed at different temperatures.

It is clearly shown from Fig. 1(a) that the film annealed at  $550^\circ\text{C}$  has amorphous structure; while the film annealed at  $600^\circ\text{C}$ , crystallizes into the perovskite phase of  $\text{SrZrO}_3$  with polycrystalline structure. It reveals that the Pt surface can enhance the nucleation of the  $\text{SrZrO}_3$  film, and the phenomenon is observed for other materials annealing on Pt coating [12]. With further increase in annealing temperature, XRD results from those films annealed at  $650$ ,  $700$  and  $750^\circ\text{C}$  indicate that these films have polycrystalline structure. The peaks from  $\text{SrZrO}_3$  thin films are indexed to be the orthorhombic (Pnma) perovskite structure with the lattice constant of  $a = 5.814 \text{ \AA}$ ,  $b = 8.196 \text{ \AA}$ , and  $c = 5.792 \text{ \AA}$ . Meanwhile, it is worth to note that with the increase of annealing temperature higher than  $600^\circ\text{C}$ , the diffraction peaks of  $\text{TiO}_2$ , caused by the interdiffusion of the Pt/Ti bottom electrode [13,14], appear which indicates that  $\text{TiO}_2$  exists at the Pt polycrystalline surface.

On the contrary as shown in Fig. 1(b), by using Pt/ $\text{TiO}_2$ / $\text{SiO}_2$ /Si substrate, even after  $800^\circ\text{C}$  annealing, there is no  $\text{TiO}_2$  peaks existed, which indicates that no  $\text{TiO}_2$  exists at the Pt polycrystalline surface. Hence the  $\text{TiO}_2$

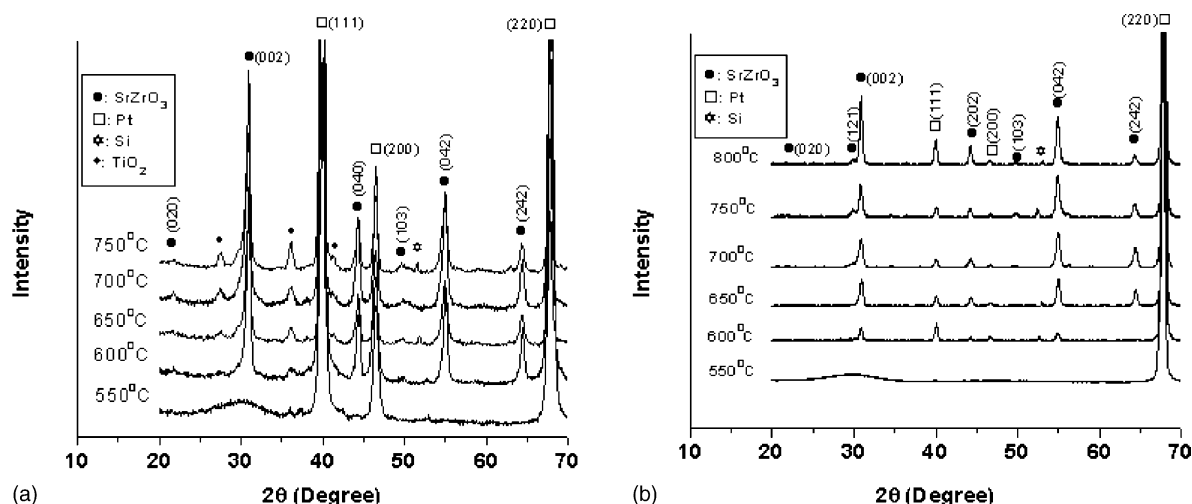


Fig. 1. X-ray diffraction patterns of  $\text{SrZrO}_3$  films on (a) Pt/Ti/ $\text{SiO}_2$ /Si substrate; and (b) Pt/ $\text{TiO}_2$ / $\text{SiO}_2$ /Si substrate.

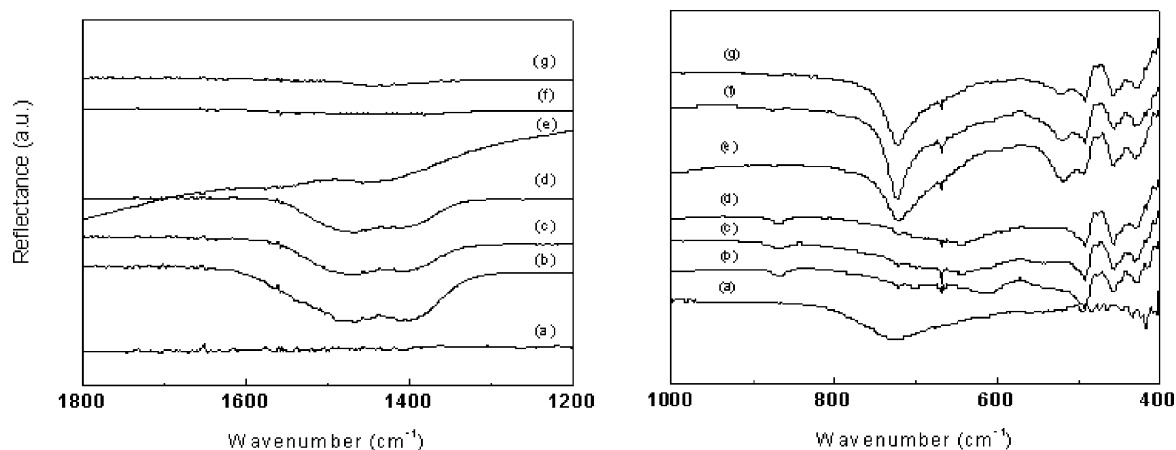


Fig. 2. FT-IR reflectivity spectra for (a)  $\text{ZrO}_2$  and annealed films deposited on  $\text{Pt/TiO}_2/\text{SiO}_2/\text{Si}$  substrate and post-annealed in  $\text{O}_2$  at (b)  $550^\circ\text{C}$ ; (c)  $600^\circ\text{C}$ ; (d)  $650^\circ\text{C}$ ; (e)  $700^\circ\text{C}$ ; (f)  $750^\circ\text{C}$ , and (g)  $800^\circ\text{C}$ .

bonding layer effectively protects the bottom electrode from the interdiffusion of Pt/Ti.

Fig. 2 shows the FT-IR reflectivity spectra of those annealed  $\text{SrZrO}_3$  films on  $\text{Pt/TiO}_2/\text{SiO}_2/\text{Si}$  substrate at  $1800\text{--}1200$  and  $1000\text{--}400\text{ cm}^{-1}$ .

There are three interesting bands for determining the phase transformation from the carbonate decomposition to the growth of the perovskite phase in the films. One is focused on the modes of metal oxygen vibrating at  $400\text{--}800\text{ cm}^{-1}$ , and the others are the modes of carbon–oxygen (C–O) vibrating at  $1300\text{--}1600\text{ cm}^{-1}$  and approximately at  $870\text{ cm}^{-1}$ . In Fig. 2, referring to the thin film annealed at  $550^\circ\text{C}$ , a shoulder band at  $1440\text{ cm}^{-1}$  and a sharp band at  $866\text{ cm}^{-1}$  associated with carbonate are observed. This fact indicates that the residual carbonate exists in the film annealed at  $550^\circ\text{C}$ ; therefore, further increase in annealing temperature is necessary to make the carbonate completely decomposed and to develop the crystallinity of the perovskite phase in these films. When the films were annealed at higher temperatures, the corresponding results shown in Fig. 2 indicate that only a very small spectral activity from these bands associated with the carbonate. And it was found that when annealed at above  $650^\circ\text{C}$ , the carbonate was completely decomposed. Meanwhile, as the increase of the annealing temperature, the perovskite

structure is developed. The spectral peaks at  $724\text{ cm}^{-1}$  is attributable to  $\text{ZrO}_6$  octahedral stretching vibration, which can be confirmed by the  $\text{ZrO}_2$  spectral peak at  $723\text{ cm}^{-1}$ . And the band at  $520\text{ cm}^{-1}$  is also attributable to  $\text{ZrO}_6$  stretching vibration [15].

Surface morphology of the films deposited on the  $\text{Pt/TiO}_2/\text{SiO}_2/\text{Si}$  substrate was investigated by scanning electron microscopy (SEM). As shown in Fig. 3, films annealed at  $600^\circ\text{C}$  were consisted of tiny vague crystal grains and were smooth and compact. And with the increase of the annealing temperature, the crystallinity of films is improved and the grain sizes increase greatly. Furthermore, the amorphous phase deflection still exists even after annealed in the furnace at  $800^\circ\text{C}$ .

### 3.2. Electrical properties

Fig. 4 shows the  $I\text{--}V$  curves of the  $\text{SrZrO}_3$  thin films. It can be clearly seen that the films deposited on the  $\text{Pt/Ti/SiO}_2/\text{Si}$  substrate show much poorer current properties compared to the films deposited on  $\text{Pt/TiO}_2/\text{SiO}_2/\text{Si}$  substrate when annealed above  $650^\circ\text{C}$ . The possible reason which has been discussed before is because the interdiffusion of the Pt/Ti bottom electrode. By using  $\text{TiO}_2$  as the bonding layer, we can effectively reduce the interdiffusion.

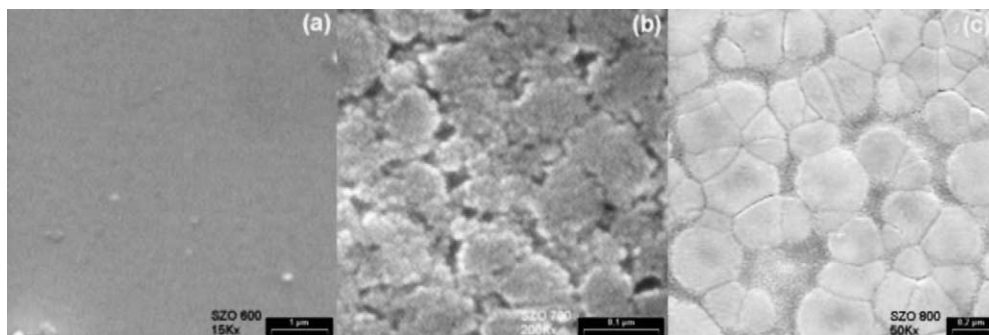


Fig. 3. SEM images of the films annealed at different temperatures: (a)  $600^\circ\text{C}$ ; (b)  $700^\circ\text{C}$  and (c)  $800^\circ\text{C}$ .

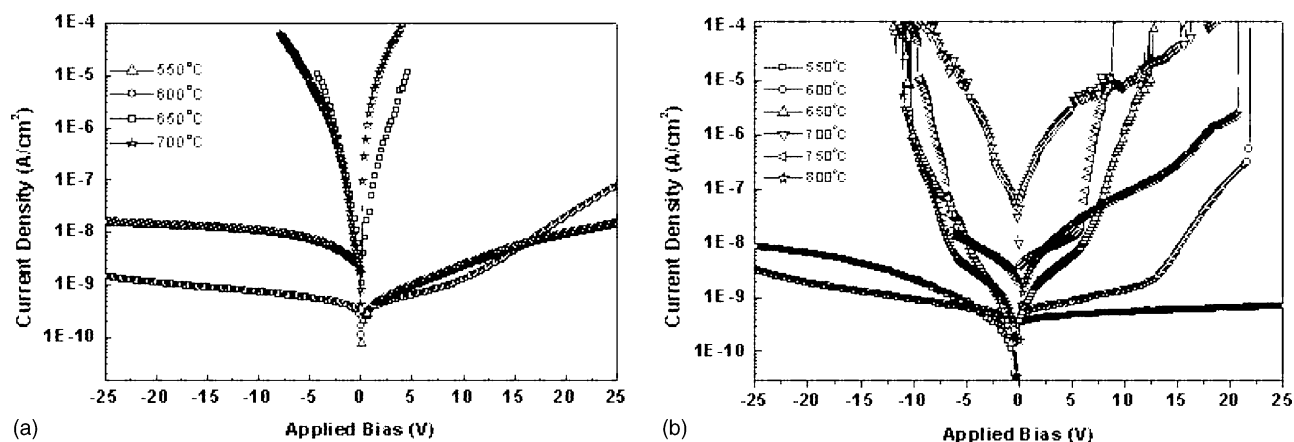


Fig. 4.  $I$ - $V$  curves of  $\text{SrZrO}_3$  thin films deposited on (a)  $\text{Pt/Ti/SiO}_2/\text{Si}$  and (b)  $\text{Pt/TiO}_2/\text{SiO}_2/\text{Si}$  substrate annealed at different temperatures.

As seen in both  $I$ - $V$  curves in Fig. 4, when annealed at 550 and 600 °C, the thin films achieve very low leakage current density at a level of  $10^{-9}$  A/cm<sup>2</sup> and high breakdown strength. The poorest current property in the films using  $\text{Pt/Ti/SiO}_2/\text{Si}$  substrate annealed above 650 °C is due to the breakdown of the bottom electrode during the annealing process. Thus it cannot be used to study the electric property of the crystalline  $\text{SrZrO}_3$ .

Meanwhile, if using  $\text{Pt/TiO}_2/\text{SiO}_2/\text{Si}$  as the substrate, the bottom electrode can survive even after annealed at 800 °C. The leakage current density of these thin films annealed at 800 °C is  $4 \times 10^{-7}$  A/cm<sup>2</sup> at a high electrical field of 1 MV/cm<sup>2</sup>. In Fig. 4(b), with the increase of annealing temperature, the current property first deteriorates which can be attributed to the increase of the undeveloped electrical defects as the films change from amorphous to polycrystalline structure. However, the thin films annealed at 800 °C show much better current property compared to those annealed at 650, 700, and 750 °C. The possible reason is that such a high-temperature treatment can greatly eliminate the electrical defects caused by the phase change after annealing.

The dielectric properties of  $\text{SrZrO}_3$  thin films annealed at different temperatures, as a function of sweeping frequency were measured at room temperature. During the measurement, the applied dc bias was zero and oscillation level was 50 mV. Fig. 5 shows the results. The very flat curves, describing the sweeping frequency dependence of the calculated dielectric constants, exhibit very little dispersion of the dielectric constants for these thin films in a frequency range from 100 Hz to 1 MHz. With the structure changing from amorphous to polycrystalline, the dielectric constant also increases from 23 to 49, indicating that crystallization can greatly affect the value of the dielectric constant.

The change of dielectric constant at room temperature, relative to the applied dc bias, was also measured using a HP 4284A LCR Meter. During the measurement, the oscillation level was 50 mV and the frequency was 100 kHz. Fig. 6 shows the dielectric constants dependence on the applied dc biases for the samples annealed at different temperatures. The flat curves with no significant changes in the dielectric constants indicate that the thin films have their dielectric constant nearly independent of the applied dc bias. Thus, in

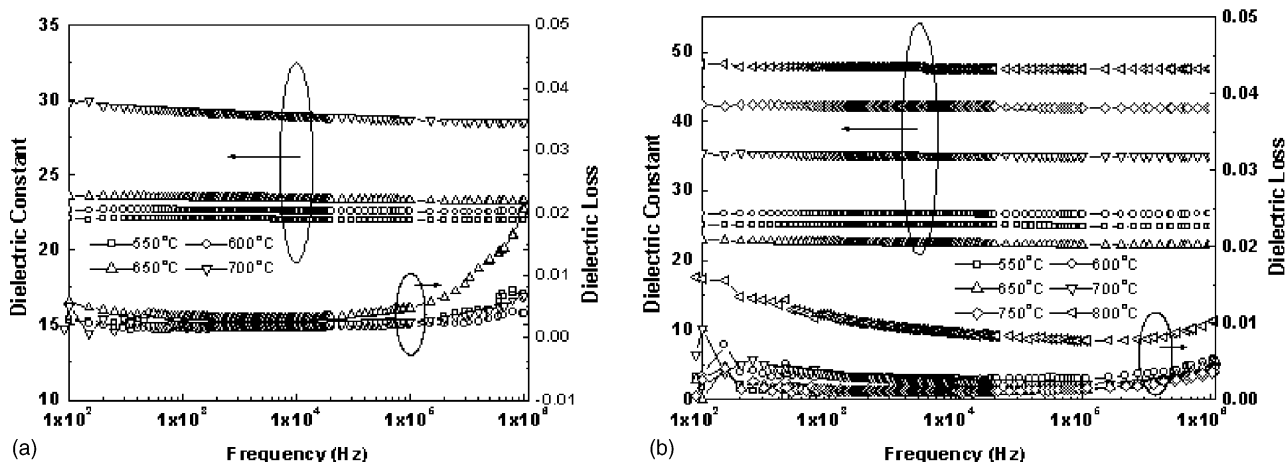


Fig. 5. Dielectric constant and dielectric loss dependence on frequency of the  $\text{SrZrO}_3$  films annealed at different temperatures in  $\text{O}_2$  deposited on (a)  $\text{Pt/Ti/SiO}_2/\text{Si}$  substrate and (b)  $\text{Pt/TiO}_2/\text{SiO}_2/\text{Si}$  substrate.

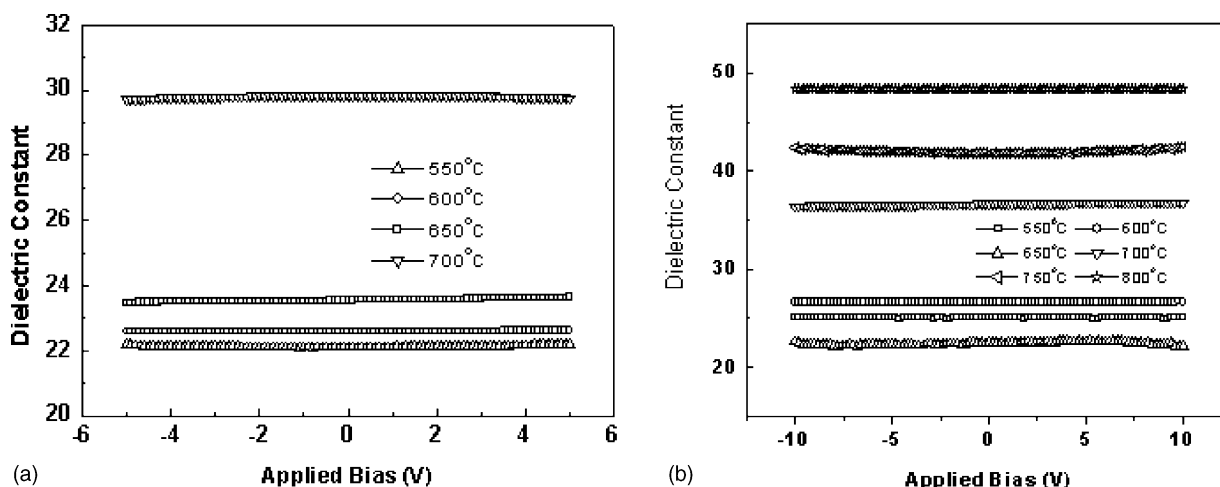


Fig. 6. Dielectric constant dependence on applied bias of the  $\text{SrZrO}_3$  films annealed at different temperatures in  $\text{O}_2$  deposited on (a) Pt/Ti/SiO<sub>2</sub>/Si substrate and (b) Pt/TiO<sub>2</sub>/SiO<sub>2</sub>/Si substrate.

this point,  $\text{SrZrO}_3$  thin films prepared by MOD technique are suitable for capacitor in practical device use which requires no practical change in the value of capacitance with the change in electric field.

#### 4. Conclusions

The effect of bottom electrodes with Pt/Ti and Pt/TiO<sub>2</sub> on the microstructures, crystalline phases and electrical properties of  $\text{SrZrO}_3$  thin films has been investigated. It has been found that when annealed above 650 °C the films deposited on Pt/TiO<sub>2</sub>/SiO<sub>2</sub>/Si substrate show much better leakage properties compared with those using Pt/Ti/SiO<sub>2</sub>/Si due to the survivor of the bottom electrode after such a heat treatment. And even annealed at 800 °C, the films deposited on Pt/TiO<sub>2</sub>/SiO<sub>2</sub>/Si substrate still have good leakage properties.

#### References

- [1] H. Iwahara, T. Esaka, H. Uchida, N. Maeda, *Solid State Ionics* 3/4 (1981) 359.
- [2] H. Iwahara, in: P. Colomban (Ed.), *Proton Conductors*, Cambridge University Press, Cambridge, UK, 1992, p. 511.
- [3] A.M. Anthony, M. Foex, in: *Proceedings of the Symposium on Magnetic Hydrodynamic Electrical Power*, vol. 3, National Agency for International Publication Inc., New York, 1966, p. 265.
- [4] T. Noguchi, T. Okubo, O. Yonemochi, *J. Am. Ceram. Soc.* 52 (1969) 4178.
- [5] C.H. Chen, W. Zhu, T. Yu, X.F. Chen, X. Yao, *Appl. Surf. Sci.* 211 (1–4) (2003) 244.
- [6] D.P. Vijay, S.B. Desu, *J. Electrochem. Soc.* 140 (1993) 2640.
- [7] H. Maiwa, N. Ichinose, K. Okazaki, *J. Appl. Phys.* 33 (1994) 5223.
- [8] R. Bruchhaus, D. Pitzer, O. Eibl, U. Scheithauer, W. Hoesler, *Res. Soc. Symp. Proc.* 243 (1992) 123.
- [9] K.H. Park, C.Y. Kim, Y.W. Jeong, H.J. Kwon, K.Y. Kim, J.S. Lee, S.T. Kim, *J. Mater. Res.* 10 (1995) 1790.
- [10] T.C. Tisone, J. Drobek, *J. Vac. Sci. Technol.* 9 (1971) 271.
- [11] K. Sreenivas, I. Reaney, T. Maeder, N. Setter, *J. Appl. Phys.* 75 (1993) 232.
- [12] W. Zhu, O.K. Tan, X. Yao, *J. Appl. Phys.* 84 (1998) 5134.
- [13] J.S. Lee, H.J. Kwon, Y.W. Jeong, H.H. Kim, K.H. Park, C.Y. Kim, *Mater. Res. Soc. Symp.* 433 (1996) 175.
- [14] H.J. Nam, H.H. Kim, W.J. Lee, *Jpn. J. Appl. Phys.* 37 (1998) 3462.
- [15] C.H. Perry, D.J. McCarthy, G. Rupprecht, *Phys. Rev.* 138 (1965) 1537.